Pure & Appl. Chem., Vol. 64, No. 11, pp. 1697–1702, 1992.
Printed in Great Britain.

Experimental methods of particle characterization

Ronald H. Ottewill

School of Chemistry, University of Bristol, Bristol BS8 1TS, England

Abstract - A recent powerful method for the characterization of particles in colloidal dispersions is provided by small angle neutron scattering. The application of this technique for the examination of particle size, particle size distributions, adsorbed layers and particle-particle interactions is described.

INTRODUCTION

Dispersions of particles with a size in the colloidal domain (ca. 1 nm to 1 μm) occur widely in industry, in biology and indeed in everyday life. Their properties can differ greatly depending on concentration, particle size, particle shape, additives present and the nature of the forces acting between the particles (ref. 1). Thus the characterization of dispersions is a subject of major importance. The definition of what is required in terms of characterization depends on the investigator and the subsequent use of the material. However, characterization requirements would typically include, particle size (mean or modal), distribution of particle sizes, surface area, particle morphology, particle shape, extent of adsorption of surfactants or polymeric species, the nature of the interactions controlling the physical behaviour of the dispersion (ref. 2).

In this contribution I will draw attention to a technique which has been developed extensively in recent years and which provides a powerful means of examining colloidal dispersions in the fluid state (ref. 3). This is small angle neutron scattering. As with all scattering techniques, e.g. those employing light, X-rays or neutrons, the neutron beam is, in general, non-destructive and by defining a scattering volume with the beam a good statistical distribution of particles can be examined. The scattered signals generated by the particles, particularly with angular variation, contain a substantial amount of information about the time-average (ref. 4) and dynamic behaviour of the system (ref. 5). A key problem is interpretation of this information. In the case of small angle neutron scattering the advantages include the following:-

i) the wavelength used is typically between 5 and 20 Å. This is of the order of or smaller than the size range of many colloidal particles. Thus considerable variation occurs in the scattered intensity as a function of scattering angle;

ii) the difference between the scattering cross-sections of hydrogen and deuterium is significantly different. Hence selective deuteration of parts of molecules and particles enables the scattering from these parts to be distinguished and thus enables structural information to be obtained. Also by the use of mixtures of hydrogenated and deuterated solvents considerable variation in scattering can be obtained which significantly helps the basic analysis of data;

iii) the neutron beam has considerable penetrating power and is insensitive to the colour of the sample.

THE TECHNIQUES OF SMALL ANGLE NEUTRON SCATTERING

The basis of a neutron scattering experiment is illustrated schematically in Fig. 1. When the neutrons are generated in a reactor the primary beam passes through a velocity selector which determines the wavelength of the beam and the spread of wavelengths. After collimation with the neutron guides the beam passes through the sample,

often contained in a quartz cuvette, and reaches the beam stop. The neutrons scattered by the sample at various angles reach the multi-detector. The latter is an extremely important part of the instrument, and usually consists of a 64 x 64 array of detector cells, i.e. in total 4096 cells. The neutrons captured by the cells are converted into electrical pulses which can be registered on computer hardware for subsequent analysis. For isotropic samples the results can be radially averaged, with each radius on the detector corresponding to a value of the scattering angle θ. Any anisotropy of scattering by the sample is readily detected in the 2-dimensional array of data. The range of θ values can be adjusted by changing the sample-detector distance. Frequently, a material such as water which has considerable incoherent scattering from the H-atoms and gives a constant intensity profile as a function of θ is used as a standard substance to convert the scattered intensity into absolute units, the number of neutrons scattered per unit of time per steradian. For elastic scattering the magnitude of the scattering vector is defined by the quantity

$$Q = 4\pi \sin(\theta/2)/\lambda$$

where λ is the wavelength of the incident beam.

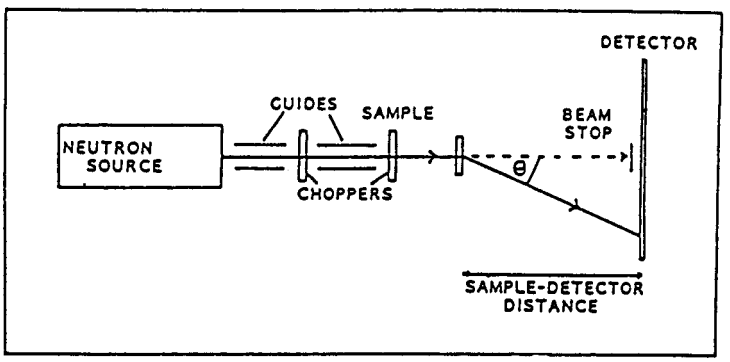

Fig. 1. Layout of a small angle neutron scattering apparatus

For a dispersion of homogeneous spherical particles, each of volume V_p, with N_p particles per unit volume the intensity of scattering, $I(Q)$, is given by (ref. 6),

$$I(Q) = A(\rho_p - \rho_m)^2 N_p V_p^2 P(Q) \qquad (1)$$

with A = an instrumental constant required to convert $I(Q)$ to absolute units, ρ_p = the coherent scattering length density of the particles and ρ_m = the coherent scattering length density of the medium. $P(Q)$ is the single particle scattering function given by (ref. 7),

$$P(Q) = \left[3(\sin QR - QR \cos QR) / (QR)^3\right]^2 = \frac{I(Q)}{I(Q=0)}$$

with R = the particle radius, so that $V_p = 4\pi R^3/3$; we note also that the volume fraction of the dispersion, ϕ, is given by $N_p V_p$. The values of coherent scattering lengths for molecules can be calculated directly from the coherent scattering lengths of the isotopic atomic constituents; the values are independent of θ and λ. Some typical values are given in Table 1 which illustrate the differences between hydrogenated and deuterated compounds.

TABLE 1. Coherent scattering length densities for molecules

Molecule	$\rho/10^{10}$ cm^{-2}
Water, H_2O	-0.56
Deuterium oxide, D_2O	6.40
h-Polystyrene, $(C_8H_8)_n$	1.41
d-Polystyrene, $(C_8D_8)_n$	6.47

PARTICLE SIZE DETERMINATION—"HOMOGENEOUS" PARTICLES

Experimental results obtained on polystyrene latices containing particles with number average diameters of 34.6 nm, 132.0 nm and 202.0 nm (ref. 8) are shown in Fig. 2. The results are plotted in the form $\ell n\ P(Q)$ against Q and hence the plots are normalised at Q = 0. The experimental data show distinct maxima and minima providing an indication of the narrow distribution of particle sizes in the samples. It should be noted that as the particle size increases, there is a shift of the curves towards the ordinate. However, most colloidal dispersions are not monodisperse and hence in order to fit the experimental data polydispersity has to be introduced into equation (1). There are various approaches to this problem and Gaussian, Schultz and log-normal distributions are often used. The zeroth-order log-normal distribution is a convenient one for computational fitting of data and can be used in the form (ref. 9,10),

$$p(R) = \frac{\exp[-(\ell n\ R - \ell n\ R_m)^2 / 2\sigma_o^2}{(2\pi)^{\frac{1}{2}}\ \sigma_o\ R_m\ \exp(\sigma_o^2/2)} \qquad (2)$$

where R_m = the modal radius of the particles and σ_o is a parameter which gives the width of the distribution. For a narrow distribution the shape is Gaussian and the standard deviation $\sigma_d = \sigma_o R_m$. Equation (2) can readily be combined with equation (1) in order to fit experimental data as shown in Fig. 2 (continuous line) giving, R_m = 17.3 nm, σ_d = 11%, R_m = 71.0 nm, σ_d = 4% and R_m = 101.0 nm, σ_d = 4%. A comparison between the particle size distribution curves obtained by small angle neutron scattering and transmission electron microscopy is shown in Fig. 3.

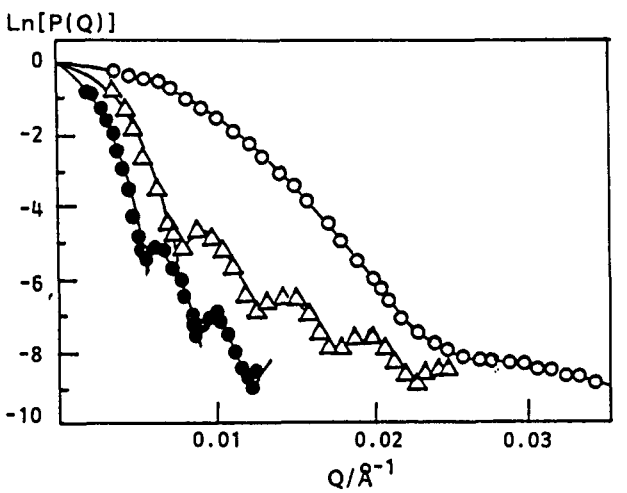

Fig. 2. $\ell n\ P(Q)$ against Q for polystyrene particles of various radii; ○, R_m = 173 Å σ_d = 11%; △, R_m = 710 Å, σ_d = 4%; ●, R_m = 1919 Å, σ_d = 4%, ——, fitted curve.

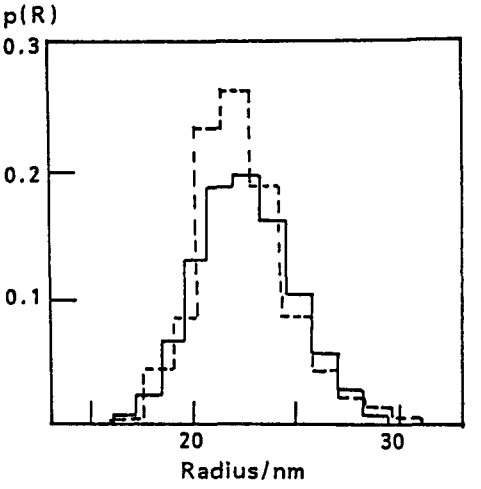

Fig. 3. Particle size distribution, ——, small angle neutron scattering, - - - -, transmission electron microscopy, R_m = 228 Å, σ_d = 11%.

PARTICLE MORPHOLOGY—NON HOMOGENEOUS PARTICLE

In many samples encountered in colloid science the particles are not homogeneous - a typical example being the situation in which the particles have an adsorbed layer of a surfactant or a polymeric species. This gives theoretically the case of a concentric sphere particle where a shell of one material surrounds a spherical core particle. Thus the core particle, of radius R_1, can be composed of a material of coherent scattering length ρ_c, and be surrounded by a shell of thickness, R_2-R_1, of coherent scattering

length, ρ_s. If the composite particle is dispersed in a medium of scattering length, ρ_m, the scattered intensity is given by (ref. 11)

$$I(Q) = A N_p [(\rho_s - \rho_m)(A_2 - A_1) + (\rho_c - \rho_m) A_1]^2 \quad (3)$$

with $A_2 = 3 V_T [(\sin QR_2 - QR_2 \cos QR_2)/Q^3 R_2^3]$

and $A_1 = 3 V_c [(\sin QR_1 - QR_1 \cos QR_1)/Q^3 R_1^3]$

Also, $V_T = 4\pi R_2^3 / 3$ and $V_c = 4\pi R_1^3 / 3$.

One of the unique opportunities which is provided by neutron scattering is that with an appropriate mixture of deuterated and hydrogenated solvents ρ_m can be made zero. We then obtain,

$$I(Q) = A N_p [(\rho_c - \rho_s) A_1 + \rho_s A_2]^2$$

Additionally, extrapolation of the experimental data to Q = O can usually be carried out by plotting $\ell n\, I(Q)$ against Q^2 giving $\ell n\, I\ (Q = O)$ and hence,

$$I(Q = O) = A N_p [\rho_s V_s + \rho_c V_c]^2$$

Further simplification (refs. 8,12,13) shows that

$$\rho_s V_s = n_s b_s$$

where n_s = the number of molecules in the shell and b_s the scattering length of the adsorbed molecules. Thus, if $[I(Q) \to O)]_c$ is obtained for the bare particle and $[I(Q = O)]_{c+s}$ for the particle with the shell, both for $\rho_m = O$ then,

$$n_s = \frac{V_c \rho_c}{b_s} \left\{ \frac{[I(Q = O)]_{c+s}^{\frac{1}{2}}}{[I(Q = O)]_c^{\frac{1}{2}}} - 1 \right\}$$

Since R_1 is also determined from experiments on the core particle, the surface area is available, and hence the amount adsorbed can be obtained. An adsorption isotherm obtained by this method for the nonionic surfactant, decyl pentaoxy ethylene glycol monoether is shown in Fig. 4. The plateau region of the isotherm corresponds to a surface excess of 2.34×10^{-10} mol cm^{-2} corresponding to an area per molecule of 70 $Å^2$.

In many cases the colloid stability of the dispersion is dependent on the presence of an attached layer and hence the core particle cannot be examined independently. However, in this case, equation (3) with variation of ρ_m can be employed to obtain both the shell thickness and the amount adsorbed (refs. 10 and 11).

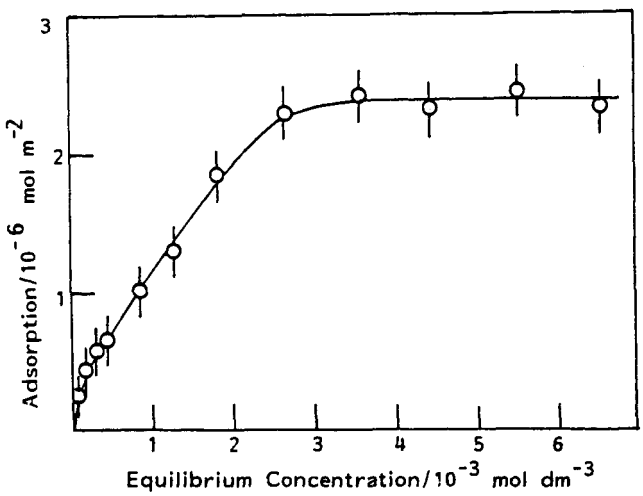

Fig. 4. Adsorption isotherm for decylpentaoxyethylene glycol monoether on polystyrene at 25°C

CHARACTERIZATION OF PARTICLE–PARTICLE INTERACTIONS

In dilute dispersions of colloidal particles the number concentration is usually low and hence interactions between particles occur rather infrequently. In concentrated dispersions, however, the particles are in constant interaction and consequently an ordering of the particles occurs which is dependent on the number concentration and the strength of the repulsive interactions. The spatial correlations which occur as a consequence of the interactions lead to interparticle interference effects which can be incorporated into equation (1) as a structure factor, S(Q), to give

$$I(Q) = A(\rho_p - \rho_m)^2 V_p \phi P(Q) S(Q)$$

where S(Q) is given by,

$$S(Q) = 1 + \frac{4\pi N_p}{Q} \int_0^\infty [g(r) - 1] \sin Qr \, dr$$

where g(r) = the pair-correlation function and r = the centre to centre interparticle separation. Hence, for well-defined monodisperse particles since P(Q) and the other parameters are well-defined S(Q) can be obtained as a function of Q and thence by Fourier transformation the pair-correlation function obtained,

$$g(r) = 1 + \frac{1}{2\pi^2 r N_p} \int_0^\infty [S(Q) - 1] Q \sin Qr \, dQ$$

The form of g(r) against r depends markedly on the type of interaction occurring between the particles. In the case of electrostatically stabilised particles, the interactions are repulsive and long-range at low electrolyte concentrations and short range at higher electrolyte concentrations. Thus at electrolyte concentrations of the order of 10^{-4} mol dm^{-3} with small particles (R = 155 Å) ordering begins to occur at quite low volume fractions. This is clearly indicated by the plot of g(r) against r results shown in Fig. 5. At the lowest volume fraction an excluded volume region is apparent and then g(r) approaches unity; this suggests the dispersion is behaving rather like a gas. At a volume fraction of 0.04 a strong first peak is apparent which increases in amplitude when the volume fraction is increased to 0.13. With increase in r the peak amplitudes decay thus indicating the presence in these systems of short-range order and long-range disorder (ref. 14).

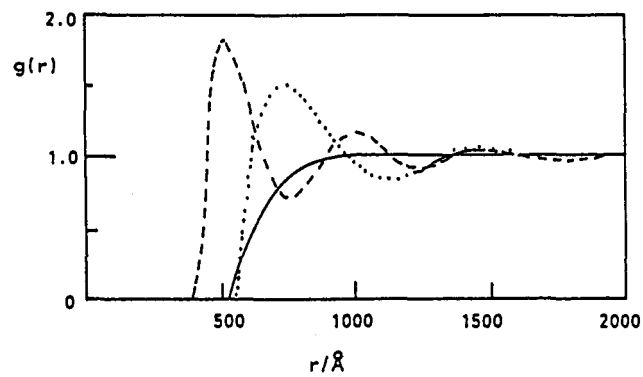

Fig.5. g(r) against r for spherical polystyrene particles, radius = 155 Å, in 10^{-4} mol dm^{-3} sodium chloride at various volume fractions, ——— , 0.01: ••••••, 0.04; – – – , 0.13.

In the case of sterically stabilised particles, such as those with a core of polymethyl methacrylate and a stabilising layer of poly-12-hydroxy stearic acid the interaction is very close to that of a hard sphere (ref. 15), in other words, interaction does not occur until the outer shells come into contact. In this case as shown in Fig. 6, substantially higher volume fractions are needed before significant ordering starts to occur for particles of approximately similar radius.

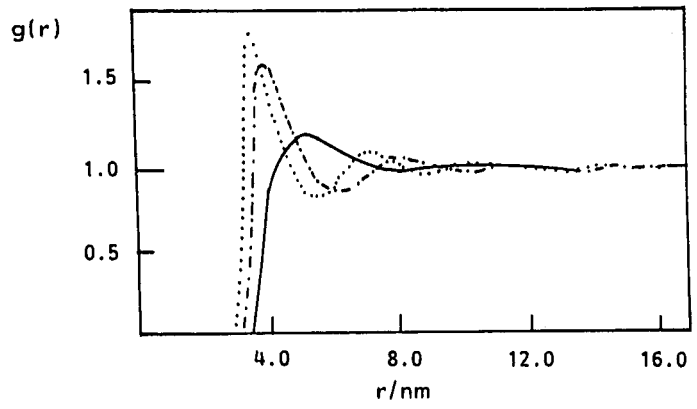

Fig. 6. g(r) against r for polymethylmethacrylate particles, behaving as nearly hard spheres, at various volume fractions, ——— , 0.23; — · — , 0.36; ····· , 0.42.

Experiments of this type are currently helping to identify the form of the pair potentials which are important for the characterization of the interactions between particles in concentrated dispersions. It is also now apparent that these dispersions form excellent models for studying the behaviour of physical states, e.g. by analogy, gaseous, fluid and crystalline and hence also the phase changes which correspond to changes of state.

REFERENCES

1. R.H. Ottewill, Future Directions in Polymer Colloids, Eds. M.S. El Aasser and R.M. Fitch, p. 253-275, Martinus Nijhoff, Dordrecht (1987).
2. J.W. Goodwin and R.H. Ottewill, J. Chem. Soc. Faraday Trans. 87, 357-369 (1991).
3. R.H. Ottewill, Colloidal Dispersions, Ed. J.W. Goodwin, p.143-163; p. 197-217, Royal Society of Chemistry, London (1981).
4. B. Cabanne, Colloides et Interfaces, p. 101-180, Eds. A.M. Cazabat and M. Veyssie, Les Editions de Physique, Z.I. de Courtaboeuf, B.P. 112, France (1983).
5. J.B. Hayter, R.H. Ottewill and P.N. Pusey, Physics of Amphiphiles, Micelles, Vesicles and Microemulsions, p. 793-801, Eds. V. Degiorgio and M. Corti, North Holland, Amsterdam (1985).
6. B. Jacrot, Rep. Prog. Phys. 39, 911-953 (1976).
7. A. Guinier and G. Fournet, Small-Angle Scattering of X-rays, p. 19, Chapman and Hall, London (1955).
8. R.H. Ottewill, Scientific Methods for the Study of Polymer Colloids and their Applications, p. 349-372, Eds. F. Candau and R.H. Ottewill, Kluwer Academic, Dordrecht (1990).
9. W.F. Espenschied, M. Kerker and E. Matijević, J. Phys. Chem. 68, 3093-3097 (1964).
10. I. Marković and R.H. Ottewill, Colloid and Polym. Sci., 264, 65-76 (1986).
11. I. Marković, R.H. Ottewill, D.J. Cebula, I. Field and J.F. Marsh, Colloid Polym. Sci., 262, 648-656 (1984).
12. N.M. Harris, R.H. Ottewill and J.W. White, Adsorption from Solution, p. 139-154, Eds. R.H. Ottewill, C.H. Rochester and A.L. Smith, Academic Press, London (1983).
13. N.M. Harris, D. Phil. thesis, University of Oxford (1980).
14. D.J. Cebula, J.W. Goodwin, G.C. Jeffrey, R.H. Ottewill, A. Parentich and R.A. Richardson, Faraday Discuss. Chem. Soc., 76, 37-52 (1983).
15. I. Marković, R.H. Ottewill, S.M. Underwood and Th.F. Tadros, Langmuir, 2, 625-630 (1986).